Tungsten oxide nanostructures: controllable growth and field emission*

Yue Shuanglin(岳双林)†, Xu Tingting(许婷婷), Li Wei(李伟), Yan Ji(闫佶), and Yi He(一禾)

Key Laboratory for Physics and Chemistry of Nanodevices, Department of Electronics, Peking University, Beijing 100871, China

Abstract: Non-fully oxidized tungsten oxide (WO_{3-x}) nanostructures with controllable morphology were fabricated by adjusting the gas pressure in chemical vapor deposition. The comparative field emission (FE) measurements showed that the obtained $W_{18}O_{49}$ nanowires have excellent FE property. The turn-on field was 7.1 V/μm for 10 μA/cm^2 and the observed highest current density was 4.05 mA/cm^2 at a field of 17.2 V/μm. Good electron emission reproducibility was also observed during thermal evaporation and desorption testing.

Key words: non-fully oxidized tungsten oxides; field emission; nanowire

DOI: 10.1088/1674-4926/33/6/063002 **PACC:** 8160C; 7970

1. Introduction

Transition metal oxides, such as tungsten oxide, are attracting increasing attention due to their promising physical and chemical properties. Among which, non-fully oxidized tungsten oxides (WO_{3-x}) are of particular interest because they may have various novel or enhanced properties, such as field-emission, gas sensing, electrochromic, optical and photocatalytic properties[1−5]. Furthermore, it has been found that tungsten oxide might be a semiconductor, a conductor or a superconductor in different oxidization states and the imperfect structures within the nonstoichiometric tungsten oxides lead to properties that could be highly valuable in many potential applications[6−8]. For this reason, controlled formation of tungsten oxides with different crystal structure, morphology and dimension is important in feasibility requirements. Over the past decades, much effort has been devoted to their syntheses. Diversified methods for tungsten oxide nanostructure preparation can be found in the literature[9−13]. However, some challenges are still faced. For example, to the best of our knowledge, investigations of the morphology and crystal structure evolution are rarely reported. Herein, we report the formation of WO_{3-x} nanostructures using a common tube furnace. Systematic studies of the process conditions were done to investigate the influence of temperature, gas pressure, growth time, and gas mixture on the morphology, crystal structure and dimension of the tungsten oxides. Comparative studies on the field emission properties of the obtained nanostructures were also conducted.

2. Experiments

First, a 20-nm-thick Au catalyst was sputtered onto the silicon substrates. After ultrasonic treatment using commercially available tungsten powders in ethanol, the obtained suspension was dropped onto these silicon substrates and baked on a hot plate. Then, the substrates were transferred into a 25 mm inner-diameter quartz tube that was inserted in a horizontal tube furnace, where one could adjust the temperature, pressure and evaporation time.

The furnace was evacuated to a base pressure of 1–5 Pa. A three-step process was taken, which involved a heating phase, followed by a growth phase and then slow cooling to room temperature. In the heating phase, the temperature was ramped to a certain degree (650–950 ℃ in our experiment) within 40 min in a gas flow of 100 sccm of Ar and 40 sccm of H_2. In the growth phase, the temperature was held at the setting degree in a mixture of 40 sccm of H_2 and 100–400 sccm of CH_4 for 30–60 min. Finally, the samples were cooled to room temperature in a gas flow of 100 sccm of Ar.

The obtained nanostructures were then dispersed in acetone by ultrasonic treatment and deposited on copper grids coated with thin carbon film for energy-dispersive X-ray spectroscopy (EDX) characterizations in a transmission electron microscope (TEM) chamber. Field emission measurements were performed in a vacuum system at a background pressure of 2.0×10^{-6} Pa, which was obtained using a turbo-pumped system. The measured sample was positioned opposite to the metal anode and the distance between them could be adjusted from 100 μm to 1 mm.

3. Results and discussion

One of the *in situ* EDX spectroscopies conducted on the obtained nanostructures is shown in Fig. 1. It demonstrates that there are only oxygen and tungsten elements in the nanostructures. The Cu and C signals come from the supporting grid. Because of the overlap between the tungsten and oxygen peaks, the ratio of tungsten to oxygen cannot be determined. From EDX characterization, no Au element was detected on the nanowires, bundles and tungsten powders. This indicates that the growth of nanostructures is not based on a vapor liquid solid (VLS) growth mechanism. One possible driving force for nanostructure growth is interfacial strain which was proposed

* Project supported by National Natural Science Foundation of China (Nos. 61106073, 60971003, 60925003) and the Key Laboratory of Photochemical Conversion and Optoelectronic Materials, TIPC, CAS (No. PCOM201021).

† Corresponding author. Email: shlyue@pku.edu.cn

Received 2 December 2011, revised manuscript received 12 January 2012

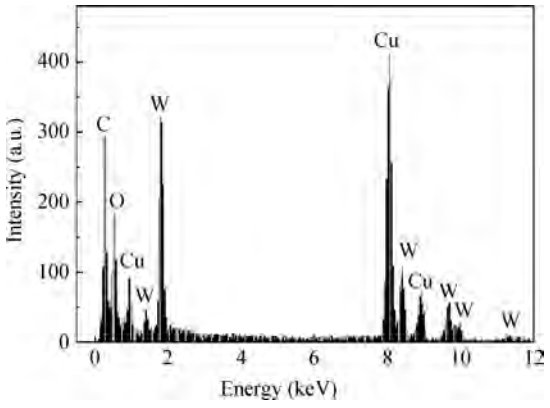

Fig. 1. One of EDX spectroscopies of the obtained tungsten oxides.

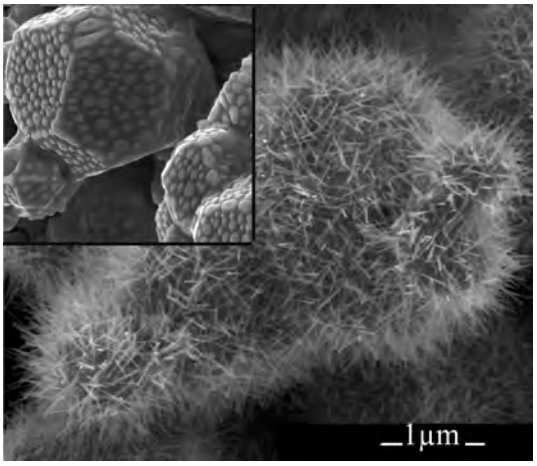

Fig. 2. SEM image of tungsten oxide nanowires grown at 760–780 ℃, the inset is SEM image of products grown in the temperature region above 780 ℃.

in Ref. [14].

Systematic studies show that temperature (650–950 ℃) somewhat influences the length and crystal structure of the products. Fixing the gas mixture at 40 sccm of H_2 and 100 sccm of CH_4, high yield nanowires are observed within 650 to 780 ℃. Figure 2(a) shows an SEM image of the nanowires grown at 760–780 ℃ for 45 min with diameters of 10–30 nm and lengths of 100–600 nm. Above 780 ℃, tungsten oxide nanowires begin to melt, as shown in the inset of Fig. 2. The corresponding XRD results exhibit that some new phase of WO_2 (JCPDs card: 02-0414) occurs (see Fig. 3(a)) besides the product of $WO_{2.83}$ (JCPDs card: 36-0103) mainly formed at lower temperatures (see Fig. 3(b)). During characterization, it was found that the length of nanowires grown in the lower temperature region is significantly shorter than that in the higher temperature region. Extending the duration of the growth time could not distinctively increase the length of the nanowires.

Varying the methane/hydrogen ratio of gas mixture from 2.5 : 1 to 10 : 1 has no significant influence on crystal structure. However, it is worth to mention that the total gas pressure is a key factor, which strongly influences the morphology of the nanostructures. When the growing gas pressure increased from 1×10^2 Pa (with a gas mixture of 40 sccm of H_2 and 100 sccm of CH_4, corresponding to Fig. 2) to 1×10^3 Pa

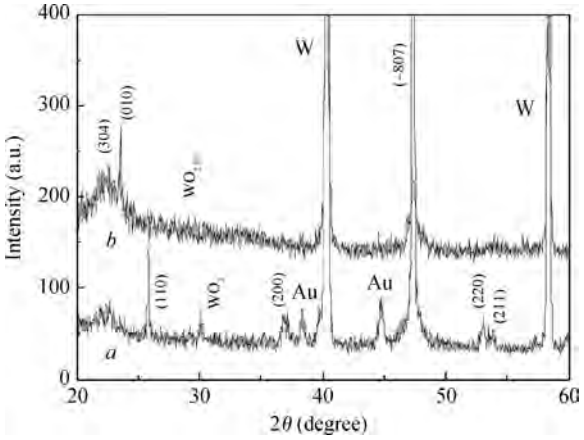

Fig. 3. XRD results of nanowires (*b*) grown at 760–780 ℃ and products (*a*) grown in the higher temperature region.

(with a gas mixture of 40 sccm of H_2 and 200 sccm of CH_4), some nanowire bundles occurred. Figure 4(a) shows the corresponding SEM image exhibiting diameters of 10–50 nm and lengths of 100–500 nm. With the gas pressure increasing to 3.2 $\times 10^3$ Pa (with a gas mixture of 40 sccm of H_2 and 200 sccm of CH_4, but adjusting the vacuum valve), more bundles appeared (see Fig. 4(b)) with widths of 10–400 nm and lengths of several microns. Most of the nanowires disappeared and were replaced by bundles (see Fig. 4(c)) of much larger width close to 1 μm when the gas pressure was adjusted to 1×10^5 Pa and then decreased to 1×10^3 Pa (with gas mixture of 40 sccm H_2 and 400 sccm of CH_4). The corresponding XRD results of Fig. 5 show that both nanowires and bundles are $W_{18}O_{49}$ (JCPDs card: 05-0392) when the gas pressure exceeded 1×10^3 Pa.

Comparative studies on the field emission properties of $W_{18}O_{49}$ nanowires and bundles show that the FE property of tungsten oxide nanowires is far better than that of bundles. For reproducibility measurement, five voltage sweeps were applied on the $W_{18}O_{49}$ nanowires (specimen in Fig. 4(a)) at different time intervals. To clearly distinguish one from another, the corresponding current density versus electric field (J–E) curves marked as 1st–5th in turn are illustrated in Figs. 6(a) and 6(b). The lowest turn-on field was 7.1 V/μm for 10 μA/cm^2 and the observed highest current density was 4.05 mA/cm^2 at a field of 17.2 V/μm. During experiments, the third sweep was immediately applied after the two voltage sweeps and from Fig. 6(a) it can be found that its J–E curve is smoother than the preceding two curves. And the turn-on electric fields for the proceeding two sweeps are lower than that in the third sweep. This can be ascribed to thermal desorption of the adsorbates on the emitters' surface in the original two voltage sweeps, which can also be verified by the phenomenon that the curves for both the first and second sweeps drop abruptly and overlap with the third curve in the high-electric field range. In a similar way, the fourth sweep was conducted several hours later. Expressly noted, its emitting current is higher than that measured in the third sweep in the high-electric field range, which might result from a slight change in morphology of the emitting tips after the high current of 4.05 mA/cm^2 emitting from the nanowires in the third measurement. The result that the emission current

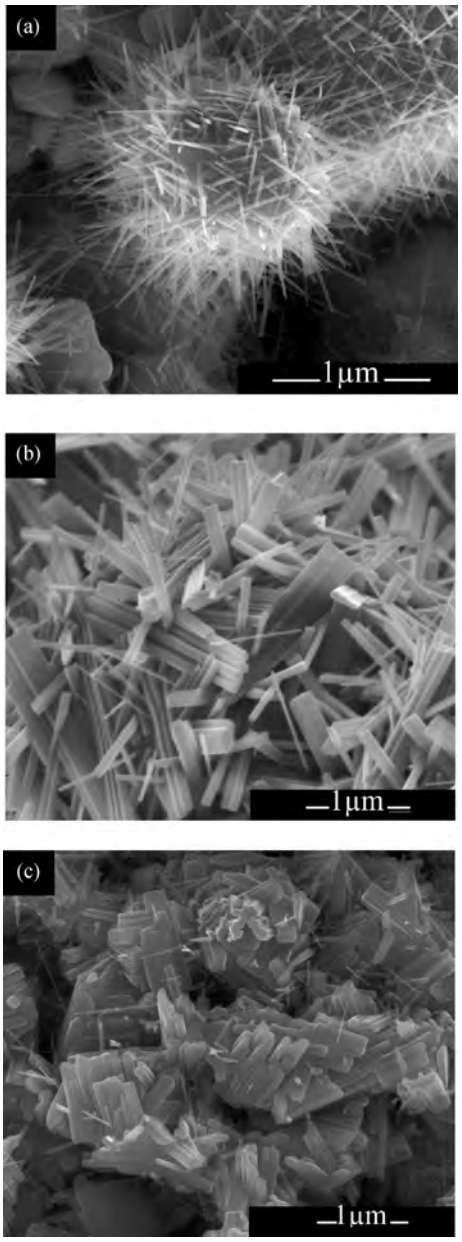

Fig. 4. Evolution of the morphology of the tungsten oxide nanostructures grown at different gas pressures, gas mixtures and growth times. (a) 1×10^3 Pa, 40 sccm H_2/200 sccm CH_4, 30 min. (b) 3.2×10^3 Pa, 40 sccm H_2/200 sccm CH_4, 60 min. (c) 1×10^5 Pa and then decreased to 1×10^3 Pa, 40 sccm H_2 /400 sccm CH_4, 30 min.

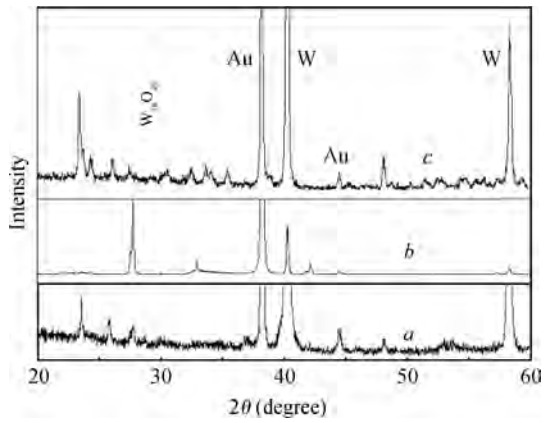

Fig. 5. The corresponding XRD results of nanostructures in Fig. 4.

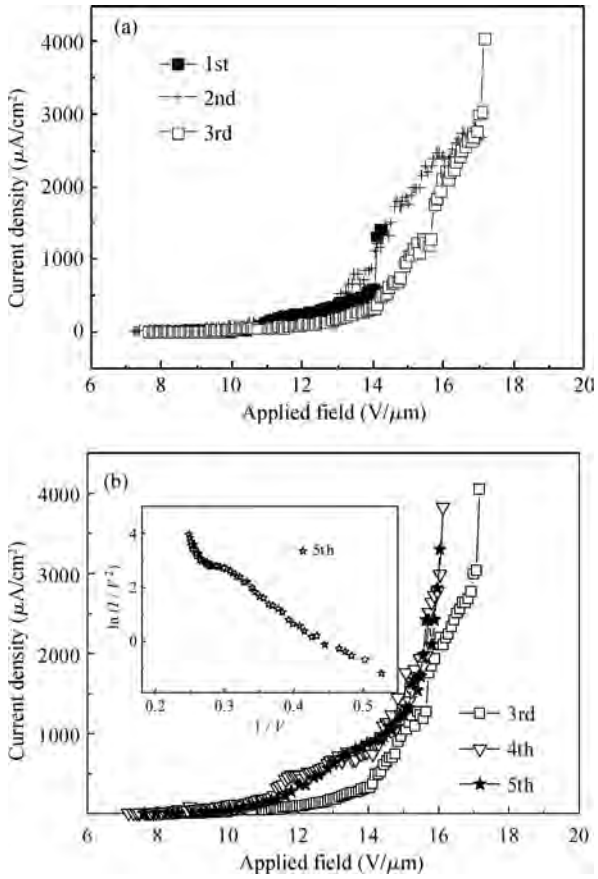

Fig. 6. Typical emission currents versus five voltage sweeps applied on tungsten oxide nanowires at different time intervals (1st–3rd are shown in part (a) and 3rd–5th are shown in part (b)), the inset of part (b) is the FN plot corresponding to the fifth measured result.

in the fifth sweep is very close to that in the fourth sweep shows that the testing sample has good electron emission reproducibility after several voltage sweeps.

The inset in Fig. 6(b) shows the FN plot of $\ln(I/V^2)$ versus $1/V$ corresponding to the fifth measured result. No current saturation is observed within the whole testing voltage sweep, which indicates that tungsten oxide nanowires might have some practical applications in high current electron sources or flat-panel displays.

4. Conclusion

In summary, tungsten oxide nanostructures were prepared under different chemical vapor deposition conditions. High yield nanowires or bundles could be obtained within 650 to 780 ℃. Above 780 ℃, tungsten oxide started to melt and a new crystal structure occurred. Extending the duration of the growth time could not remarkably alter the length of the nanostructures. Varying the methane/hydrogen ratio of the gas mixture from 2.5 : 1 to 10 : 1 had no significant influence on the formation of tungsten oxide. However, it was found that the gas pressure had a strong influence on the morphology of the nanostructures and had some effect on the crystal struc-

ture. The XRD results showed that both nanowires and bundles were $W_{18}O_{49}$ phase when the gas pressure exceeded 1 $\times 10^3$ Pa. The field emission measurements showed that the $W_{18}O_{49}$ nanowires have good electron emission reproducibility and high emission current.

References

[1] Liu F, Mo F Y, Jin S Y, et al. A novel lift-off method for fabricating patterned and vertically-aligned $W_{18}O_{49}$ nanowire arrays with good field emission performance. Nanoscale, 2011, 3: 1850

[2] Qin Y X, Hu M, Zhang J. Microstructure characterization and NO_2-sensing properties of tungsten oxide nanostructures. Sens Actuators B, 2010, 150: 339

[3] Chang X T, Sun S B, Li Z J, et al. Assembly of tungsten oxide nanobundles and their electrochromic properties. Appl Surf Sci, 2011, 257: 5726

[4] Guo C S, Yin S, Huang Y F, et al. Synthesis of $W_{18}O_{49}$ nanorod via ammonium tungsten oxide and its interesting optical properties. Langmuir, 2011, 27: 12172

[5] Sun S B, Chang X T, Dong L H, et al. $W_{18}O_{49}$ nanorods decorated with Ag/AgCl nanoparticles as highly-sensitive gas-sensing material and visible-light-driven photocatalyst. J Solid State Chem, 2011, 184: 2190

[6] Salje E K H. Polarons and bipolarons in tungsten-oxide WO_{3-x}. J Eur Solid State Inorg Chem, 1994, 3: 805

[7] Aird A, Domeneghetti M C, Mazzi F, et al. Sheet superconductivity in WO_{3-x}: crystal structure of the tetragonal matrix. J Phys: Condens Matter, 1998, 10: L569

[8] Zhao H W, Hua Z Q, Li T Y, et al. Origin of varistor properties of tungsten trioxide (WO_3) ceramics. J Semicond, 2010, 31: 023001

[9] Hong K Q, Xie M H, Hu R, et al. Diameter control of tungsten oxide nanowires as grown by thermal evaporation. Nanotechnology, 2008, 19: 085604

[10] Huang R, Zhu J, Yu R. Synthesis and electrical characterization of tungsten oxide nanowires. Chin Phys B, 2009, 18: 3024

[11] Cui S M, Lu G H, Mao S, et al. One-dimensional tungsten oxide growth through a grain-by-grain buildup process. Chem Phys Lett, 2010, 485: 64

[12] You L, Sun Y F, Ma J, et al. Highly sensitive NO_2 sensor based on square-like tungsten oxide prepared with hydrothermal treatment. Sens Actuators B-Chem, 2011, 157: 401

[13] Fang F, Kennedy J, Futter J, et al. Size-controlled synthesis and gas sensing application of tungsten oxide nanostructures produced by arc discharge. Nanotechnology, 2011, 22: 335702

[14] Klinke C, Hannon J B, Gignac L, et al. Tungsten oxide nanowire growth by chemically induced strain. J Phys Chem B, 2005,109: 17787